

## Direct band gaps in multiferroic h-LuFeO<sub>3</sub>

B. S. Holinsworth, D. Mazumdar, C. M. Brooks, J. A. Mundy, H. Das, J. G. Cherian, S. A. McGill, C. J. Fennie, D. G. Schlom, and J. L. Musfeldt

Citation: [Applied Physics Letters](#) **106**, 082902 (2015); doi: 10.1063/1.4908246

View online: <http://dx.doi.org/10.1063/1.4908246>

View Table of Contents: <http://scitation.aip.org/content/aip/journal/apl/106/8?ver=pdfcov>

Published by the [AIP Publishing](#)

---

### Articles you may be interested in

[Room temperature multiferroicity in orthorhombic LuFeO<sub>3</sub>](#)

Appl. Phys. Lett. **105**, 052911 (2014); 10.1063/1.4892664

[The adsorption-controlled growth of LuFe<sub>2</sub>O<sub>4</sub> by molecular-beam epitaxy](#)

Appl. Phys. Lett. **101**, 132907 (2012); 10.1063/1.4755765

[Spin-charge-orbital coupling in multiferroic LuFe<sub>2</sub>O<sub>4</sub> thin films](#)

Appl. Phys. Lett. **100**, 212904 (2012); 10.1063/1.4720401

[Optical properties and electronic structure of multiferroic hexagonal orthoferrites RFeO<sub>3</sub> \(R=Ho, Er, Lu\)](#)

J. Appl. Phys. **111**, 056105 (2012); 10.1063/1.3693588

[Preparation and photoabsorption characterization of Bi Fe O<sub>3</sub> nanowires](#)

Appl. Phys. Lett. **89**, 102506 (2006); 10.1063/1.2345825

---

The advertisement features a photograph of the Lake Shore Model 372 cryogenic temperature controller on the left, which is a white rectangular device with a digital display and a keypad. On the right, there is a detailed, artistic rendering of a cryogenic system's internal components, including a large cylindrical dewar, various pipes, and a complex network of brass and stainless steel parts. The background is a gradient of blue and white, suggesting a cold environment.

Precise temperature control  
for **cryogenic research**

**Model 372**

**Lake Shore**  
CRYOTRONICS



## Direct band gaps in multiferroic $h$ -LuFeO<sub>3</sub>

B. S. Holinsworth,<sup>1</sup> D. Mazumdar,<sup>1,a)</sup> C. M. Brooks,<sup>2</sup> J. A. Mundy,<sup>3</sup> H. Das,<sup>3</sup> J. G. Cheriai,<sup>1,4</sup> S. A. McGill,<sup>4</sup> C. J. Fennie,<sup>3</sup> D. G. Schlom,<sup>2,5</sup> and J. L. Musfeldt<sup>1</sup>

<sup>1</sup>Department of Chemistry, University of Tennessee, Knoxville, Tennessee 37996, USA

<sup>2</sup>Department of Material Science and Engineering, Cornell University, Ithaca, New York 14853, USA

<sup>3</sup>School of Applied and Engineering Physics, Cornell University, Ithaca, New York 14853, USA

<sup>4</sup>National High Magnetic Field Laboratory, Tallahassee, Florida 32310, USA

<sup>5</sup>Kavli Institute at Cornell for Nanoscale Science, Ithaca, New York 14853, USA

(Received 9 January 2015; accepted 30 January 2015; published online 23 February 2015)

We measured the optical properties of epitaxial thin films of the metastable hexagonal polymorph of LuFeO<sub>3</sub> by absorption spectroscopy, magnetic circular dichroism, and photoconductivity. Comparison with complementary electronic structure calculations reveals a 1.1 eV direct gap involving hybridized Fe 3d<sub>2</sub> + O 2p<sub>z</sub> → Fe d excitations at the  $\Gamma$  and A points, with a higher energy direct gap at 2.0 eV. Both charge gaps nicely overlap the solar spectrum. © 2015 AIP Publishing LLC. [<http://dx.doi.org/10.1063/1.4908246>]

High temperature multiferroics with strong magneto-electric coupling are immensely desirable for magnetic memory, tunable filtering, and medical/biotechnology applications.<sup>1</sup> Single phase materials have, however, proven elusive, at least under a classical definition where they must be simultaneously ferroelectric and ferromagnetic.<sup>2,3</sup> Once the description was broadened to include other forms of magnetism,<sup>4</sup> viable candidates including BiFeO<sub>3</sub> and TbMnO<sub>3</sub> emerged.<sup>5–8</sup> Further broadening to include field-induced multiferroics led to the inclusion of CuO and hexaferrites.<sup>9,10</sup> What distinguishes these compounds is their ability to overcome the contradictory requirements for ferroelectricity and magnetism, albeit by different mechanisms and with various degrees of cross-coupling. One of these candidates,  $h$ -LuFeO<sub>3</sub>, was originally thought to be a room temperature multiferroic.<sup>11</sup> This system has hexagonal symmetry with space group  $P6_3cm$  in epitaxially stabilized thin films. It is ferroelectric below 1020 K and a non-collinear antiferromagnet below 147 K.<sup>12</sup> This system is a derivative of LuFe<sub>2</sub>O<sub>4</sub>, which has a fascinating phase diagram<sup>13,14</sup> that emanates from the interplay between charge, structure, and magnetism.

In this letter, we bring together optical absorption spectroscopy, magnetic circular dichroism, photoconductivity, and first principles calculations to reveal the electronic structure of  $h$ -LuFeO<sub>3</sub>. Surprisingly, we uncover direct gaps at both 1.1 and 2.0 eV, different than previously supposed.<sup>21</sup> The 1.1 eV feature, which we assign as hybridized Fe 3d<sub>2</sub> + O 2p<sub>z</sub> → Fe d excitations, is challenging to identify due to its modest intensity which derives from the low density of states (DOS). The 2.0 eV direct gap is stronger and arises from  $p$ - $d$  charge-transfer excitations. It displays a 10 meV jump through the Néel temperature due to spin-charge coupling. That said, the overall absorption coefficient in  $h$ -LuFeO<sub>3</sub> is lower than that in many other complex oxides like LuFe<sub>2</sub>O<sub>4</sub> and BiFeO<sub>3</sub>. This difference emanates from the fact that the valence states are primarily in the spin-up channel whereas

the conduction states are mostly in the spin-down channel. As a result of the gap hierarchies and relatively high magnetic ordering temperature,  $h$ -LuFeO<sub>3</sub> may find applications beyond light harvesting in sensing and flash memory devices.

High quality epitaxial LuFeO<sub>3</sub> films were grown at 800 °C on (111)-orientated yttria-stabilized zirconia substrates using molecular-beam epitaxy,<sup>12</sup> and film quality was assessed by x-ray diffraction and susceptibility. Optical measurements were carried out using a Perkin-Elmer  $\lambda$ -900 spectrometer (0.41–6.53 eV) in both transmittance and reflectance modes, and the absorption [ $\alpha(E)$ ] was determined via combined Glover-Tinkham and Kramers-Kronig techniques.<sup>15</sup> Magnetic circular dichroism was performed at the National High Magnetic Field Laboratory, Tallahassee, using the Split-Florida Helix magnet up to 30 T (Ref. 16). The dichroic signal was determined from the ratio of the photoelastic modulator and beam chopper responses, respectively. Photoconductivity was performed on a custom-made setup that included a Xenon lamp, contact tips, picoammeter, and power meter, along with a series of narrow bandpass filters and a sputtering system for deposition of 250  $\mu$ m Pt contacts. First principles calculations were performed using the density functional theory +  $U$  method including spin-orbit coupling, as implemented in the full-electron WIEN2K package with  $U = 4.5$  eV and  $J = 0.95$  eV for Fe.

Figure 1(a) displays the absorption spectrum of  $h$ -LuFeO<sub>3</sub> at 4 and 300 K. The response is typical of a semiconductor. Plots of  $(\alpha \cdot E)^2$  and  $(\alpha \cdot E)^{0.5}$  vs. energy<sup>17</sup> reveal direct and indirect band gaps as

$$\alpha(E) = \frac{A}{E}(E - E_{g,dir})^{0.5} + \frac{B}{E}(E - E_{g,indir} + E_{ph})^2. \quad (1)$$

Here,  $\alpha(E)$  is the absorption coefficient,  $E_{g,dir}$  is the direct gap energy,  $E_{g,indir}$  is the indirect gap energy,  $E_{ph}$  is the phonon energy mediating any indirect gap component,  $E$  is the photon energy, and A and B are coefficients. This approach was developed for traditional semiconductors with single parabolic bands and has been extended to analyze oxides,

<sup>a)</sup>Current address: Department of Physics, Southern Illinois University, Carbondale, Illinois 62901, USA.

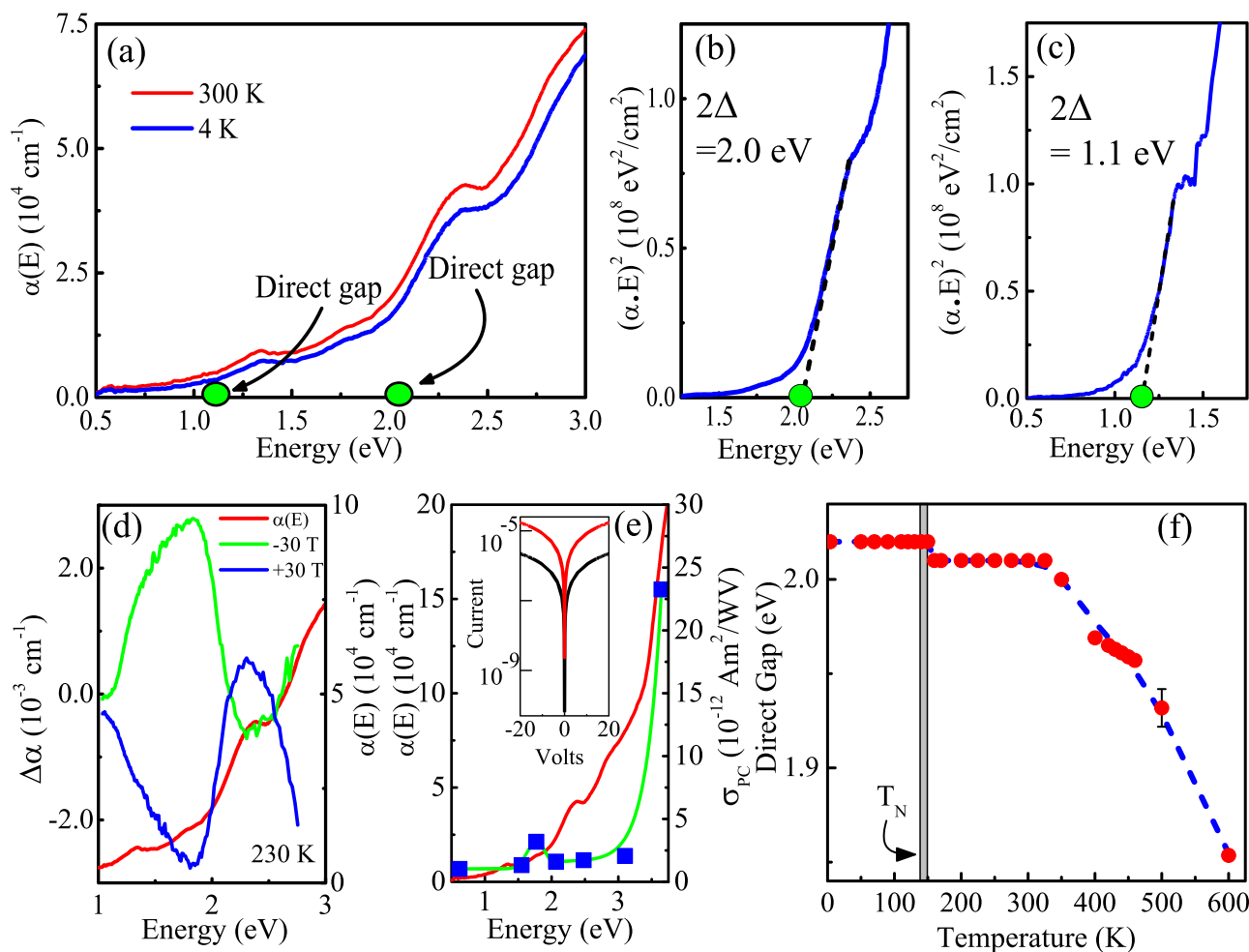


FIG. 1. (a) Absorption spectra of *h*-LuFeO<sub>3</sub> at 300 and 4 K. (b) and (c) Direct gap analysis of the 4 K data. (d) Magnetic circular dichroism in the high temperature paramagnetic phase (230 K) compared to the room temperature optical absorption. (e) Photocurrent of *h*-LuFeO<sub>3</sub> (blue squares) compared with the 300 K absorption spectrum. The green line guides the eye. The inset shows *I*-*V* curves taken with a broadband xenon source with on/off given as red:black. (f) Temperature dependence of the 2.0 eV direct gap.

despite their more complicated band structures.<sup>18–20</sup> Our analysis reveals the presence of at least two direct gaps [Figs. 1(b) and 1(c)]. Consistent with prior work, we easily identify the 2.0 eV direct gap.<sup>21</sup> The spectrum also displays a lower energy structure on top of a long near infrared tail. These features were previously assigned as impurities and multiple reflections.<sup>21</sup> However, in our analysis, we find evidence for a direct gap at 1.1 eV [Fig. 1(c)], which we assign as the fundamental gap of LuFeO<sub>3</sub>. This structure also has minor indirect character. As discussed below, a 1.1 eV gap is strikingly consistent with predictions from first principles calculations.<sup>22</sup> Interestingly, the 1.1 eV direct gap in *h*-LuFeO<sub>3</sub> is smaller than that of several other iron-containing oxides including BiFeO<sub>3</sub> (2.7 eV),<sup>23</sup> CoFe<sub>2</sub>O<sub>4</sub> (1.2 eV), NiFe<sub>2</sub>O<sub>4</sub> (1.6 eV), and LuFe<sub>2</sub>O<sub>4</sub> (~0.35 eV) are different in that they are fundamentally indirect gap materials.<sup>13,18,24–26</sup>

The left panel of Fig. 2 shows *h*-LuFeO<sub>3</sub>'s density of states, calculated in the GGA + *U* + SOC framework. The data are for the weakly ferromagnetic *A*<sub>2</sub> magnetic state which is the zero temperature ground state from theory.<sup>22</sup> Neutron diffraction data<sup>11</sup> have indicated a low temperature *A*' configuration which is nearly degenerate in energy to *A*<sub>2</sub>.<sup>22</sup> In this respect, the optical properties are expected to be similar. Our calculations show *h*-LuFeO<sub>3</sub> to be an insulator

with a band gap of 1.0 eV, consistent with the aforementioned optical absorption analysis. The valence band edge is dominated by Fe 3*d* and O *p* states, mainly in the spin-up channel. There is a natural node in the density of states near -1.6 eV that will be important in later discussion. Strongly hybridized O + Fe states are deeper, around 2 eV below the Fermi level, and they are equally populated in either channel. The conduction band edge consists of spin-down Fe 3*d* states (*d*<sub>xz</sub>, *d*<sub>yz</sub>, *d*<sub>xy</sub>, and *d*<sub>x<sup>2</sup>-y<sup>2</sup></sub> orbitals) with higher Fe 3*d*<sub>z<sup>2</sup></sub> states about 2 eV above the Fermi level. Even though crystal field theory assigns Fe<sup>3+</sup> to the high-spin *d*<sup>5</sup> state, our calculations indicate substantial down-spin Fe DOS up to the valence band edge. This allows on-site Fe *d*-*d* transitions and *p*-*d* charge transfer excitations. We identify these excitations as candidates for the fundamental gap. The 2.0 eV direct gap is primarily due to charge-transfer *p*-*d* excitations from deeper O *p* to empty Fe 3*d*. The overall low oscillator strength of the experimental absorption spectrum emanates from the fact that the valence states are mostly in the spin-up channel whereas the conduction states are principally in the spin-down channel. Even above 2.0 eV, the absorption coefficient does not rise into the usual 10<sup>5</sup> cm<sup>-1</sup> range. This is because there are very few unoccupied spin-up Fe states, which prohibit any substantial optical absorption in the spin-up

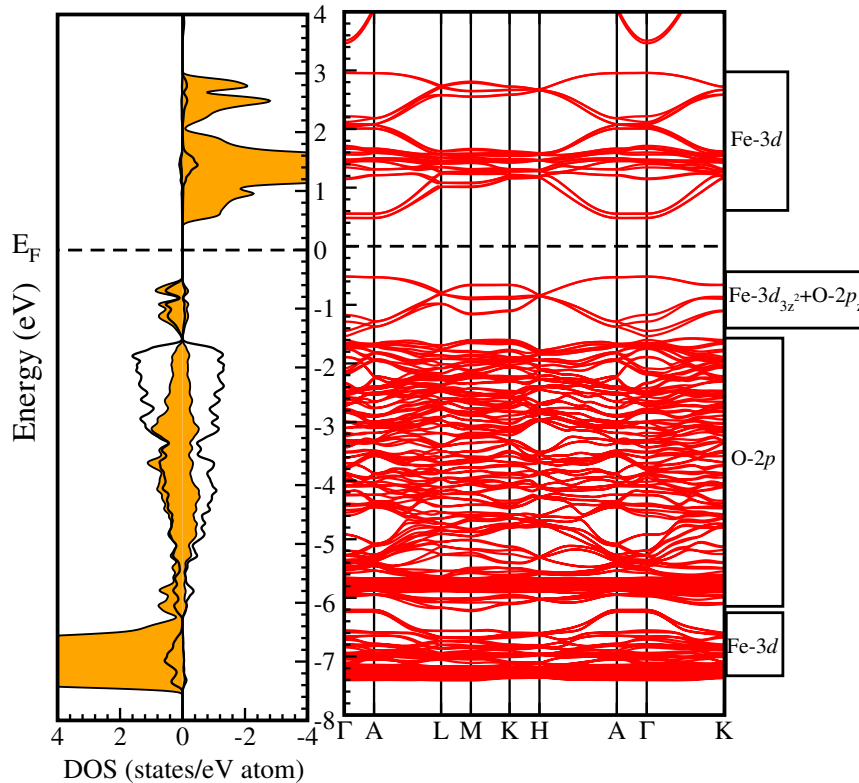


FIG. 2. Left: density of states of  $h$ -LuFeO<sub>3</sub> calculated using the GGA +  $U$  + SOC method. Right: energy bands of  $h$ -LuFeO<sub>3</sub> at high symmetry points in the Brillouin zone. A direct gap at  $\Gamma$ , A, and points between is predicted.

channel. Spin-up to spin-down transitions are formally spin-forbidden, and although spin-orbit coupling relaxes this selection rule, the probability of carrier excitation by this mechanism is relatively low.

To analyze the nature of the fundamental and higher energy gaps, we plot the GGA +  $U$  bands along certain high symmetry points, as shown in the right panel of Fig. 2. Both the valence band maximum and the conduction band minimum are flat from  $\Gamma$  to the A point of the Brillouin zone. That both bands are nearly dispersionless means that  $h$ -LuFeO<sub>3</sub> is essentially a direct gap system with a primary band gap of  $\approx 1.0$  eV. The valence band-maximum is a combination of Fe  $3d_{3z^2}$  and apical O- $2p_z$  states. Numerous nearly degenerate indirect gaps are also close to the direct gap. This observation is consistent with the partial indirect character observed for the lower gap in our optical analysis. The 2.0 eV direct gap can be assigned to  $p$ - $d$  charge-transfer excitations as well. Again, the optical absorption coefficient is low, even above 2 eV, because the valence states are primarily in the spin-up channel whereas the conduction states are mainly in the spin-down channel.

Additional evidence for a lower energy band gap in  $h$ -LuFeO<sub>3</sub> comes from magnetic circular dichroism spectra. We focussed our efforts between 1.0 and 2.75 eV, searching for evidence of electronic excitations in this region, with the expectation that any dichroic response will provide insight into the nature of the important states, both in the paramagnetic and non-collinear antiferromagnetic phases. Figure 1(d) displays the dichroic response of  $h$ -LuFeO<sub>3</sub> in the paramagnetic phase at  $\pm 30$  T ( $H \parallel k$ ) along with the room temperature optical absorption for comparison. We find a strong dichroic response throughout the investigated spectral range. One lobe peaks (dips) near 1.8 eV and is more than 1 eV

wide. After a zero-crossing near 2.1 eV, a second lobe starts to take shape. Much of this structure is well below the larger (2.0 eV) direct gap of  $h$ -LuFeO<sub>3</sub>. The presence of dichroically active features down to almost 1 eV supports our proposal for important electronic states in this region. Density of states data reveals that the dichroically active excitations involve both Fe  $d$  and Fe  $3d_{z^2} + O 2p_z$  hybridized states. As we discuss below, band structure effects are largely responsible for the shape of the dichroic response.

One prominent model for describing the dichroic characteristics of materials in their paramagnetic state<sup>27</sup> can be written as

$$\Delta\alpha_{r-l}(E) = \frac{-16\pi^3 EN}{3hc} H \left[ \frac{\mathcal{A}}{h} \frac{\partial g(E)}{\partial E} + \left( \mathcal{B} + \frac{\mathcal{C}}{k_B T} \right) g(E) \right]. \quad (2)$$

Here, differential optical absorption  $\Delta\alpha_{r-l}(E)$  depends upon  $\mathcal{A}$ ,  $\mathcal{B}$ , and  $\mathcal{C}$ . parameters that represent excited state Zeeman effects, mixing of zero-field states, and the ground state population distribution, respectively.<sup>27,29</sup> In addition,  $E$  is the energy of the photon,  $N$  is the number of unit cells per cm<sup>3</sup>,  $g(E)$  is the density of states,  $h$  is Planck's constant,  $k_B$  is Boltzmann's constant,  $c$  is the speed of light, and  $T$  is the temperature. But what accounts for the characteristic shape of the dichroic response in Fig. 1(d)? A careful look at the valence band density of states immediately reveals a mechanism. The natural node in the density of states near  $-1.6$  eV will cause  $g(E)$  to approach zero, effectively eliminating any contribution of the  $\mathcal{B}$  and  $\mathcal{C}$  terms to the dichroic response at 1.8 eV where the maxima and minima occur. At the same time, the shape of the response is driven by the derivative,  $\partial g(E)/\partial E$ . This amplifies the  $\mathcal{A}$  term and is most likely



responsible for the large peak (dip) structure in the dichroic response. In fact, it drives all three of the features in the spectrum. Therefore, we find that band structure effects (both the density of states itself and the energy derivative of this quantity) are responsible for the shape of the dichroic spectrum.<sup>28</sup>

Photoconductivity measurements provide some support for the presence of electronic states below 2.0 eV, although the evidence is not as conclusive as that from the magnetic circular dichroism. Figure 1(e) displays the photocurrent of *h*-LuFeO<sub>3</sub> taken at different energies compared with the linear absorption spectrum. *I*-*V* curves in the dark and under illumination with a broadband xenon source are also included. The photocurrent shows a small peak near 1.65 eV, in line with expectations from the optical response. This makes sense because  $\sigma_{PC} \sim \eta \cdot \alpha(E) \cdot \tau$ , where  $\sigma_{PC}$  is the photo-induced conductivity,  $\eta$  is the quantum efficiency or probability of making photocarriers,  $\alpha(E)$  is the absorption coefficient, and  $\tau$  is the photo-carrier lifetime.<sup>30</sup> The slight increased photocurrent between 1 and 2.0 eV correlates reasonably well with evidence for a lower band gap. It is also in line with the aforementioned magnetic circular dichroism work, which reveals important electronic states in this region. The photocurrent and absorption coefficient both track to significantly higher values with increasing photon energy, evidence that the most important band gap is at 2.0 eV.

Finally, we carried out variable-temperature spectroscopic measurements between 4 and 600 K, searching for optical signatures of the Néel transition. Figure 1(d) displays the temperature dependence of the 2.0 eV direct gap. It is rigid at low temperature and drops by  $\approx 10$  meV through the Néel temperature. This drop is the same order of magnitude as the exchange constant (*J*).<sup>12,31</sup> Although the band gap in *h*-LuFeO<sub>3</sub> is only weakly sensitive to the magnetic transition, the 10 meV contraction is a signature of spin-charge coupling. The gap softens above 300 K, reaching a value of 1.85 eV at 600 K. We find no evidence for spin-charge interactions near 440 K,<sup>11</sup> consistent with recent neutron diffraction.<sup>32</sup> The sensitivity of the 2.0 eV gap in *h*-LuFeO<sub>3</sub> to *T<sub>N</sub>* has interesting parallels. The gap in BiFeO<sub>3</sub> softens through the 640 K Néel transition,<sup>23</sup> that in LuFe<sub>2</sub>O<sub>4</sub> decreases through the 330 K charge ordering transition,<sup>13</sup> and that in Ni<sub>3</sub>V<sub>3</sub>O<sub>8</sub> hardens through the magnetic quantum critical transition.<sup>33</sup> By contrast, the 2.7 eV direct gap in CoFe<sub>2</sub>O<sub>4</sub> is rigid up to approximately 800 K.<sup>25</sup>

Summarizing, we brought together optical absorption, magnetic circular dichroism, and photoconductivity to investigate the electronic structure of epitaxial thin films of *h*-LuFeO<sub>3</sub> and compared our findings with complementary first principles calculations. Surprisingly, we uncover a 1.1 eV direct gap emanating from hybridized Fe 3*d*<sub>z<sup>2</sup></sub> + O 2*p*<sub>z</sub> → Fe *d* excitations in addition to the previously reported direct gap at 2.0 eV. The latter is sensitive to the magnetic ordering transition due to spin-charge coupling. The overall absorption coefficient is lower than that in many other complex oxides because the valence states are mostly in the spin-up channel whereas the conduction states are principally in the spin-down channel. The observation that the fundamental gap is lower than previously supposed can be advantageous for light

harvesting. Moreover, even with a 147 K ordering temperature, multiferroicity in *h*-LuFeO<sub>3</sub> is achieved at relatively high temperature, a characteristic that may allow fabrication of low power, voltage-controlled magnetic devices operating at liquid nitrogen temperature.

Research at Tennessee and Cornell was supported by the U.S. Department of Energy, Office of Basic Energy Sciences, Division of Materials Sciences under Award Nos. DE-FG02-01ER45885 (J.L.M.) and DE-SC0002334 (C.J.F., D.G.S., C.M.B., J.A.M., and H.D.). Some work was performed in part at the Cornell NanoScale Facility, a member of the National Nanotechnology Infrastructure Network, which is supported by the National Science Foundation (Grant ECCS-0335765). Work at National High Magnetic Field Laboratory was supported by the National Science Foundation through DMR-0084173 and the State of Florida. J.A.M. acknowledges the financial support from the Army Research Office in the form of a National Defense Science & Engineering Graduate Fellowship and from the National Science Foundation in the form of a graduate research fellowship. We thank Madalina Furis for useful discussions.

<sup>1</sup>J. M. D. Coey, *Magnetism and Magnetic Materials* (Cambridge University Press, New York, 2010), p. 555.

<sup>2</sup>H. Schmid, *Ferroelectrics* **162**, 317 (1994).

<sup>3</sup>N. Hill, *J. Phys. Chem. B* **104**, 6694 (2000).

<sup>4</sup>D. Khomskii, *Physics* **2**, 20 (2009).

<sup>5</sup>C. M. Folkman, S. H. Baek, H. W. Jang, C. B. Eom, C. T. Nelson, X. Q. Pan, Y. L. Li, L. Q. Chen, A. Kumar, V. Gopalan, and S. K. Streiffer, *Appl. Phys. Lett.* **94**, 251911 (2009).

<sup>6</sup>C. Beekman, W. Siemons, T. Z. Ward, J. D. Budai, J. Z. Tischler, R. Xu, W. Liu, N. Balke, J. H. Nam, and H. M. Christen, *Appl. Phys. Lett.* **102**, 221910 (2013).

<sup>7</sup>C. Ederer and N. Spaldin, *Phys. Rev. B* **71**, 060401 (2005).

<sup>8</sup>T. Kimura, T. Goto, H. Shintani, K. Ishizaka, T. Arima, and Y. Tokura, *Nature* **426**, 55 (2003).

<sup>9</sup>T. Kimura, Y. Sekio, H. Nakamura, T. Siegrist, and A. P. Ramirez, *Nat. Mater.* **7**, 291 (2008).

<sup>10</sup>V. V. Pavlov, A. R. Akbashev, A. M. Kalashnikova, V. A. Rusakov, A. R. Kaul, M. Bayer, and R. V. Pisarev, *J. Appl. Phys.* **111**, 056105 (2012).

<sup>11</sup>W. Wang, J. Zhao, W. Wang, Z. Gai, N. Balke, M. Chi, H. N. Lee, W. Tian, L. Zhu, X. Cheng, D. J. Keavney, J. Yi, T. Z. Ward, P. C. Snijders, H. M. Christen, W. Wu, J. Shen, and X. S. Xu, *Phys. Rev. Lett.* **110**, 237601 (2013).

<sup>12</sup>J. A. Moyer, R. Misra, J. A. Mundy, C. M. Brooks, J. T. Heron, D. A. Muller, D. G. Schlom, and P. Schiffer, *APL Mater.* **2**, 012106 (2014).

<sup>13</sup>X. S. Xu, M. Angst, T. V. Brinzari, R. P. Hermann, J. L. Musfeldt, A. D. Christianson, D. Mandrus, B. C. Sales, S. McGill, J.-W. Kim, and Z. Islam, *Phys. Rev. Lett.* **101**, 227602 (2008).

<sup>14</sup>N. Kimizuka, A. Takenaka, Y. Sasada, and T. Katsura, *Solid State Commun.* **15**, 1321 (1974).

<sup>15</sup>R. E. Glover and M. Tinkham, *Phys. Rev.* **108**, 243 (1957).

<sup>16</sup>25 T in the Split-Florida Helix at the National High Magnetic Field Laboratory refers to the magnetic field strength within the sample volume at the magnet's mid-plane location. For MCD, which requires magneto-optical Faraday geometry, we have displaced the sample slightly above the mid-plane and thereby achieve field strengths as high as 30 T.

<sup>17</sup>J. I. Pankove, *Optical Processes in Semiconductors* (Dover, New York, 1971).

<sup>18</sup>Q.-C. Sun, H. Sims, D. Mazumdar, J. X. Ma, B. S. Holinworth, K. R. O'Neal, G. Kim, W. H. Butler, A. Gupta, and J. L. Musfeldt, *Phys. Rev. B* **86**, 205106 (2012).

<sup>19</sup>K. H. Kim, K. C. Park, and D. Y. Ma, *J. Appl. Phys.* **81**, 7764 (1997).

<sup>20</sup>X. S. Xu, J. F. Ihlefeld, J. H. Lee, O. K. Ezekoye, E. Vlahos, R. Ramesh, V. Gopalan, X. Q. Pan, D. G. Schlom, and J. L. Musfeldt, *Appl. Phys. Lett.* **96**, 192901 (2010).

- <sup>21</sup>W. Wang, H. Wang, X. Xu, L. Zhu, L. He, E. Wills, X. Cheng, D. J. Keavney, J. Shen, X. Wu, and X. Xu, *Appl. Phys. Lett.* **101**, 241907 (2012).
- <sup>22</sup>H. Das, A. L. Wysocki, Y. Geng, W. Wu, and C. J. Fennie, *Nat. Commun.* **5**, 2998 (2014).
- <sup>23</sup>S. R. Basu, L. W. Martin, Y. H. Chu, M. Gajek, R. Ramesh, R. C. Rai, X. Xu, and J. L. Musfeldt, *Appl. Phys. Lett.* **92**, 091905 (2008).
- <sup>24</sup>C. M. Brooks, R. Misra, J. A. Mundy, L. A. Zhang, B. S. Holinsworth, K. R. O'Neal, T. Heeg, W. Zander, J. Schubert, J. L. Musfeldt, Z.-K. Liu, D. A. Muller, P. Schiffer, and D. G. Schlom, *Appl. Phys. Lett.* **101**, 132907 (2012).
- <sup>25</sup>B. S. Holinsworth, D. Mazumdar, H. Sims, Q.-C. Sun, M. K. Yurtisigi, S. K. Sarker, A. Gupta, W. H. Butler, and J. L. Musfeldt, *Appl. Phys. Lett.* **103**, 082406 (2013).
- <sup>26</sup>The calculated conduction bands are also more dispersive than those in the spinel ferrites.<sup>18,25</sup>
- <sup>27</sup>P. J. Stephens, *Annu. Rev. Phys. Chem.* **25**, 201 (1974).
- <sup>28</sup>First, there is a feature in the DOS around  $-0.9$  eV and from here it is  $\approx 1.5$  eV to the conduction band edge plus a rigid shift that is noted by the difference between theory and experiment (0.9 vs 1.1 eV band gap). Second, we see a feature in the DOS around  $-1.6$  eV and from here it is  $\approx 2.1$  eV to the conduction band edge, which again via the rigid shift correlates to the smaller intensity feature in the MCD. Finally, we see a sharp rise in the DOS just after the  $-1.6$  eV node. This results in a feature in the MCD that is not fully resolved but present none-the-less. If we take a qualitative look at the slopes for these three regions, we see that the first is a fairly strong slope which gives a strong intensity in the MCD response. The second is far less dispersed and thus has a significantly weaker contribution to the response. The final region has a steep slope and this is represented in the data as a significant increase in response.
- <sup>29</sup>W. R. Mason, *A Practical Guide to Magnetic Circular Dichroism Spectroscopy* (John Wiley & Sons, New Jersey, 2007).
- <sup>30</sup>*Springer Handbook of Electronic and Photonic Materials*, edited by S. Kasap and P. Capper (Springer, New York, 2006), Chap. 7, p. 137.
- <sup>31</sup>H. Wang, I. V. Solovyev, W. Wang, X. Wang, P. Ryan, D. J. Keavney, J.-W. Kim, T. Z. Ward, L. Zhu, X. M. Cheng, J. Shen, L. He, X. S. Xu, and X. Wu, *Phys. Rev. B* **90**, 059903 (2014).
- <sup>32</sup>S. M. Disseler, X. Luo, Y. S. Oh, R. Hu, D. Quintana, A. Zhang, J. W. L. S.-W. Cheong, and W. Ratcliff II, "Magnetic structure of hexagonal Mn-doped  $\text{LuFeO}_3$ " (unpublished).
- <sup>33</sup>P. Chen, B. S. Holinsworth, K. R. O'Neal, T. V. Brinzari, D. Mazumdar, Y. Q. Wang, S. McGill, R. J. Cava, B. Lorenz, and J. L. Musfeldt, *Phys. Rev. B* **89**, 165120 (2014).